Medicinal Plant Biology

ARTICLE

Open Access

https://doi.org/10.48130/mpb-0024-0033
Medicinal Plant Biology **2025**, 4: e006

Evaluation of the authenticity of Citri Grandis Exocarpium based on metabolomics and transcriptomics

Haiting Huang[1,2,3,4#], Yu Liu[1,2,3,4#], Jianmu Su[1,2,3,4], Xiangxiu Liang[1,2,3,4], Hong Wu[1,2,3,4*] and Mei Bai[1,2,3,4*]

[1] *Guangdong Technology Research Center for Traditional Chinese Veterinary Medicine and Natural Medicine, South China Agricultural University, Wushan Road, Guangzhou 510642, China*
[2] *Guangdong Laboratory for Lingnan Modern Agriculture, South China Agricultural University, Wushan Road, Guangzhou 510642, China*
[3] *Guangdong Key Laboratory for Innovative Developmentand Utilization of Forest Plant Germplasm, South China Agricultural University, Wushan Road, Guangzhou 510642, China*
[4] *Center for Medicinal Plants Research, College of Life Sciences, South China Agricultural University, Guangzhou 510642, China*
[#] Authors contributed equally: Haiting Huang, Yu Liu
[*] Corresponding authors, E-mail: wh@scau.edu.cn; baimei@scau.edu.cn

Abstract

Citri Grandis Exocarpium (CGE) is derived from the immature or nearly mature dried outer peel of *Citrus grandis* 'Tomentosa' (Huazhou pomelo) or *C. grandis* (L.) Osbeck (pomelo). CGE is a traditional medicinal herb from Guangdong Province (China) that primarily contains active substances, such as flavonoids, with expectorant, antitussive, and anti-inflammatory properties. However, the differences in quality and the mechanisms underlying these differences between the two plant sources specified in the Chinese Pharmacopoeia have not been fully elucidated. For the first time, this study systematically analyzed Huazhou pomelo (*C. grandis* 'Tomentosa') from its authentic production region and Sanhong pomelo (*C. grandis* (L.) Osbeck) from Meizhou by using an integrated analysis of metabolomics and transcriptomics. The results showed that the flavonoid components in both extracts were generally consistent, indicating that both pomelos could serve as sources of CGE. However, the content differed significantly. Flavonoids related to medicinal effects, such as naringin and hesperidin, were significantly more abundant in Huazhou pomelo than in Sanhong pomelo, with compounds such as 5-demethylnobiletin detected only in Huazhou pomelo. The integrative metabolomics and transcriptomics analysis identified 11 key structural genes and transcription factors potentially involved in flavonoid biosynthesis, providing candidate targets for functional validation. This study uncovered the molecular basis for Huazhou pomelo being superior in quality to Sanhong pomelo as an authentic medicinal material for CGE and provided scientific evidence for optimizing quality standards and enhancing its commercial value. Furthermore, this study provided a theoretical foundation for further functional research.

Citation: Huang H, Liu Y, Su J, Liang X, Wu H, et al. 2025. Evaluation of the authenticity of Citri Grandis Exocarpium based on metabolomics and transcriptomics. *Medicinal Plant Biology* 4: e006 https://doi.org/10.48130/mpb-0024-0033

Introduction

Citri Grandis Exocarpium (CGE) is made from the immature or nearly mature dried outer peel of *Citrus grandis* 'Tomentosa' (Huazhou pomelo) or *C. grandis* (L.) Osbeck (pomelo)[1]. Huazhou pomelo is a cultivated variety of pomelo that originates from Huazhou City, Guangdong Province, China. Huazhou pomelo received geographical indication protection in 2007 and was officially recorded in the 'Chinese Pharmacopoeia' as the source plant for the traditional Chinese medicine 'Citri Grandis Exocarpium'[2]. The main bioactive components of CGE are flavonoids, volatile oils, polysaccharides, and coumarins[3–5]. These components endow CGE with various pharmacological activities, including as an antioxidant, antibacterial, antitussive, expectorant, and allergic asthma treatment, and play significant roles in the prevention and treatment of COVID-19; thus, CGE has been included in treatment plans for COVID-19[6–9]. The key components of CGE are naringin, naringenin, isosinensetin, apigenin, hesperidin, and isoquercitrin, which have expectorant, antitussive, anti-inflammatory, anticancer, and antiallergic activities[9–12]. Naringin is listed as a marker component of CGE by the 'Chinese Pharmacopoeia'.

Research on different sources of CGE has mainly focused on the components in different strains of Huazhou pomelo, comparative analysis of the main components of different strains of Huazhou pomelo and different varieties of pomelo, and the main components of different parts (i.e., flowers, leaves, fruits) of different strains of Huazhou pomelo and different varieties of pomelo[2,3,13–16]. The current application of multi-omics research in medicinal plants has played a significant role in advancing the understanding of the functions of medicinal plants and their natural products, as well as the mechanisms underlying their authenticity[17–19]. Transcriptomics and metabolomics research has primarily focused on component comparisons between varieties of pomelo and Huazhou pomelo, the main components of different parts (i.e. flowers, leaves, and fruits) of the Huazhou pomelo, and screening of transcription factors and structural genes related to the flavonoid pathway[4,20–24]. Additionally, studies have explored the geoherbalism of CGE from different regions, concluding that the flavonoid composition of Huazhou pomelo from Huazhou City is similar to that of two other regions but significantly differs in content, suggesting that nobiletin, demethylnobiletin, and heptamethoxyflavone can serve as markers for the geoherbalism of CGE[1]. However, few comprehensive analyses have been conducted to determine whether the pharmacological quality of Huazhou pomelo is superior to other variates, and precise quality evaluations using advanced transcriptomics and metabolomics of Huazhou pomelo and other varieties of pomelo as sources of CGE have rarely been reported.

Therefore, this study selected Huazhou pomelos from Huazhou City, a key production area, and Sanhong pomelos from Meizhou as the experimental materials and employed combined metabolomics and transcriptomics techniques to investigate the main advantages of Huazhou pomelo as a source plant for CGE. Through untargeted

metabolomics, relative quantification of the main active components (flavonoids) in CGE was conducted and combined with HPLC techniques to analyze the main flavonoid components. Further, key differentially expressed genes in the flavonoid pathway were screened from metabolomic and transcriptomic data, and qRT-PCR was used for the relative quantification of these genes. A comprehensive assessment concluded that the main reason for Huazhou pomelo being the geoherbal source of CGE was the significantly higher content of pharmacologically active flavonoids in Huazhou pomelo than in Sanhong pomelo, particularly the presence of demethylnobiletin in Huazhou pomelo.

Materials and methods

Plant materials

The Huazhou Pomelo used in this study was selected from the Huazhou pomelo plantation located in Gou'ertang Village, Ligang Town, Huazhou City, Maoming City, Guangdong Province (21°47′4″ N 110°38′29″ E). Sanhong pomelo was selected from the pomelo plantation located in Huangmei Village, Bingcun Town, Meixian District, Meizhou City, Guangdong Province, China (24°21′27″ N 116°17′49″ E). The selected fruits were free from mechanical damage and pest characteristics, with a diameter of 7–8 cm (Fig. 1a). The outer peels of the fruits were immediately frozen in liquid nitrogen and stored at −80 °C, with another portion being freeze-dried (Christ Alpha 1-2 LD plus, Germany).

Total flavonoid extraction and HPLC quantification

From the freeze-dried outer peel powder of Huazhou pomelo or Sanhong pomelo, 0.5 g was weighed, and 15 mL of methanol was added, followed by ultrasound in a 60 °C water bath for 45 min. The mixture was centrifuged at 10,000 rpm for 10 min, and the supernatant was collected for use. Rutin was used as a reference to determine the total flavonoid content, using a multifunctional microplate reader (Tecan Infinite® 200 PRO, Switzerland) to measure absorbance at 510 nm and a quantitative relationship curve drawn between absorbance and rutin concentration. One mL of the sample flavonoid extract, diluted twice, was taken, and reagents were added according to the above steps, measuring the absorbance at 510 nm and substituting it into the rutin standard curve ($y = 2.4415x + 0.1327$, $R^2 = 0.9995$) to obtain the total flavonoid content in Huazhou pomelo and Sanhong pomelo. Each sample was repeated three times.

A high-performance liquid chromatography instrument (Agilent 1260 Infinity, USA) and an InfinityLab Poroshell 120 SB-C18 column (2.7 μm 150 mm × 4.6 mm) were used, with acetonitrile (B) and 0.1% formic acid aqueous solution (D) as the mobile phase. The gradient elution program was: 0–6 min, 25%–30% B; 6–10 min, 30%–35% B; 10–16 min, 35%–60% B; 16–18 min, 60%–80% B; 18–22 min, 80%–25% B. The injection volumes were 2 μL and 6 μL, with a flow rate of 0.8 mL/min. Flavonoids in the samples, including quercetin, naringenin chalcone, naringenin, hesperidin, narirutin, diosmin, neohesperidin, rhoifolin, sinensetin, apigenin, tangeretin, and nobiletin, were qualitatively and quantitatively analyzed at 283 and 340 nm, respectively.

Metabolomics analysis

The Huazhou pomelo and Sanhong pomelo samples were slowly thawed at 4 °C. An appropriate amount of sample (50–100 mg) was weighed, 1 mL of water : acetonitrile : isopropyl alcohol (1:1:1, v/v) was added, vortexed for 60 s, sonicated at low temperature for 30 min, centrifuged at 12,000 rpm and 4 °C for 10 min, and the supernatant was collected. The protein was precipitated at −20 °C for 1 h, centrifuged at 12,000 g and 4 °C for 10 min, and the supernatant was vacuum-dried and re-dissolved in 200 μl of 50% ACN, vortexed, centrifuged at 14,000 g and 4 °C for 15 min, and the supernatant was taken for detection.

Metabolites in the samples were detected using an Ultra-High Performance Liquid Chromatography-Electrostatic Field Orbitrap Mass Spectrometry (UHPLC-Q Exactive HFX, Thermo Scientific, USA) with a Waters HSS T3 column (100 mm × 2.1 mm, 1.8 μm); mobile phase was 0.1% formic acid-water (A) and 0.1% formic acid-acetonitrile (B); flow rate 0.3 mL/min; column temperature 40 °C; injection volume 2 μL; elution gradient: 0.0–1.0 min A/B (100:0 v/v), 1.0–9.0 min A/B (5:95 v/v), 9.0–13.0 min A/B (5:95 v/v), 13.1–17.0 min A/B (100:0 v/v); samples were kept in the autosampler at 4 °C throughout the analysis. Electrospray ionization (ESI) conditions were: sheath gas 40 arb; auxiliary gas 10 arb; spray voltage 3,000 V/−2,800 V; temperature 350 °C; ion transfer tube temperature 32 °C. The scan mode was Full-MS-ddMS2 mode, positive and negative ion scan range 70–1,050 Da, secondary scan range 200–2,000 Da, primary resolution 70,000, secondary resolution 17,500. Metabolites in the biological samples were qualitatively and quantitatively detected and subsequently analyzed by matching retention time, molecular mass (mass error < 10 ppm), and secondary fragmentation spectra with local and commercial databases.

Transcriptome sequencing

After extracting RNA from the samples, library construction, purification, and quality control were performed. Upon passing quality control, different libraries were pooled according to the effective concentration and target on-machine data volume and sequenced on the Illumina Novaseq 6000. Raw data were filtered using Fastp software to remove primer and adapter sequences, sequences with fragment lengths < 50 bp, and low-quality bases to obtain cleaned data. Q20, Q30, and GC content and sequencing error rate distribution levels were calculated. The cleaned data were aligned to the reference genome (https://db.cngb.org/search/project/CNP0002121), and the location information of reads on the reference genome and the characteristic information of sequencing samples were obtained using HISAT2[25,26]. Known and new genes and transcripts were quantified using StringTie[27]. Differential expression at the transcript and gene levels was analyzed using DEseq2[28], with the screening criteria set as $|\log2(\text{fold change})| > 1$ and Q value ≤ 0.05 after FDR correction, resulting in the identification of differentially expressed genes (DEGs).

Weighted gene co-expression network analysis (WGCNA)

Weighted gene co-expression network analysis (WGCNA) was performed using the R package WGCNA (v1.47) to describe the gene association patterns between different samples[29]. After removing genes with extremely low expression levels in all samples, the expression values of the remaining 14,844 genes were imported into WGCNA, selecting a power value of 7. The hub gene selection criteria were geneModuleMembership > 0.8 and geneTraitSignificance > 0.8.

qRT-PCR

The steps of real-time fluorescent quantitative PCR (qRT-PCR) included RNA extraction from samples, reverse transcription of RNA to cDNA, and qRT-PCR of selected genes. Total RNA from the outer peel of Huazhou pomelo and Sanhong pomelo was extracted using the FastPure® Plant Total RNA Isolation Kit (Vazyme, China), and cDNA was synthesized using the HiScript®III 1st Strand cDNA Synthesis Kit (Vazyme, China). Using *β-actin* as the reference gene, structural genes *CgPAL2*, *CgPAL8*, *Cg4CL2*, *Cg4CL6*, *CgCHS4*, *CgCHI2*, *CgF3H1*, *CgFLS1*, *CgOMT1*, *CgOMT3*, and *CgOMT5* in the flavonoid

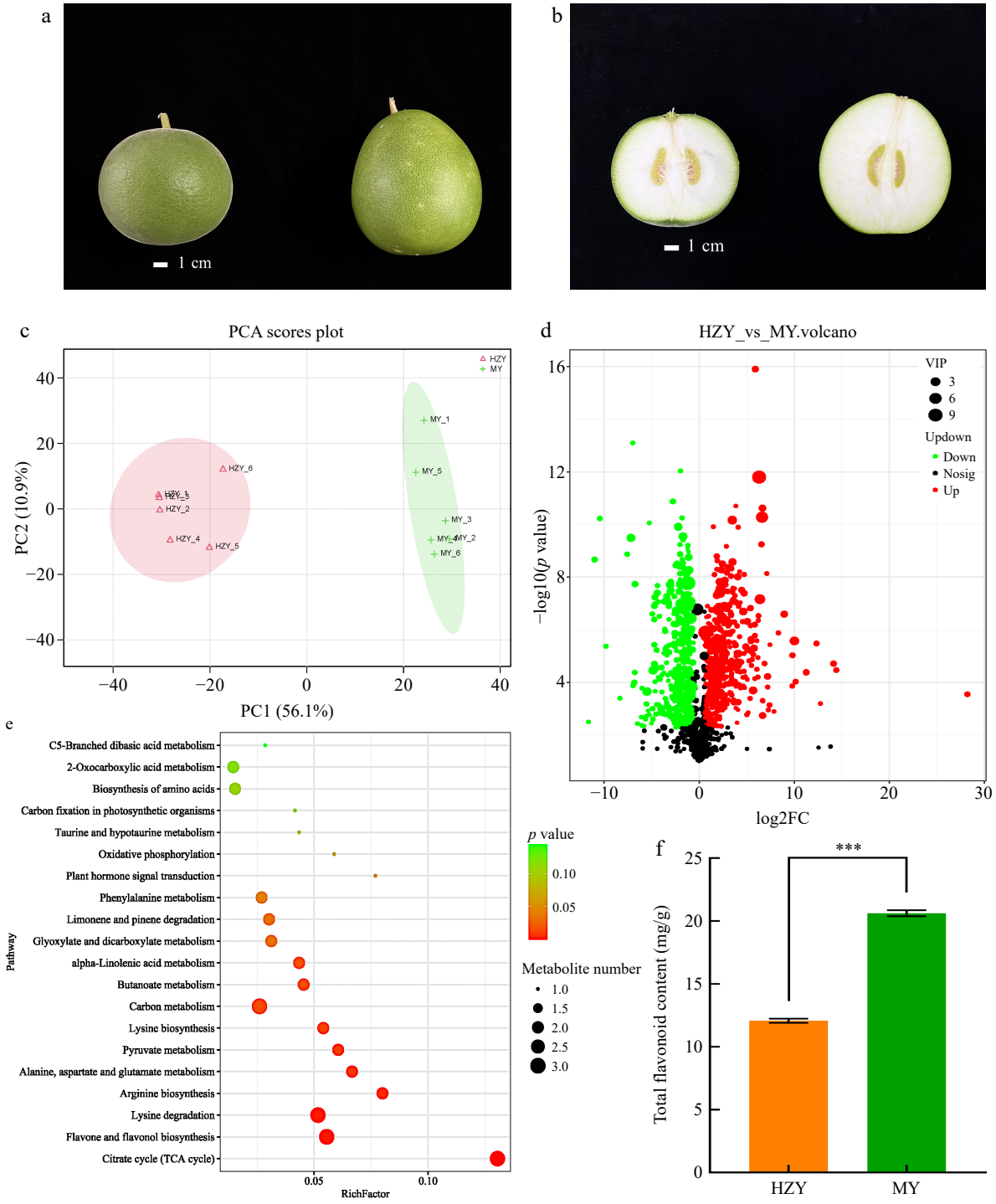

Fig. 1 Morphological and metabolomic results of Huazhou pomelo and Sanhong pomelo. (a) Morphological differences in whole fruit, with Huazhou pomelo on the left and Sanhong pomelo on the right. The Huazhou pomelo is round with a peel covered in fine white fuzz, whereas the Sanhong pomelo is oval-shaped with a relatively smooth surface. (b) Morphological differences in halved fruit, with Huazhou pomelo on the left and Sanhong pomelo on the right. The top of the Huazhou pomelo is round, blunt, and slightly concave, whereas the top of the Sanhong pomelo is flat. (c) Principal component score plot of metabolites, with HZY representing Huazhou pomelo and MY representing Sanhong pomelo (same for the following panels). (d) Volcano plot of differential metabolites, where each point represents a metabolite. Green, red, and black points represent downregulated, upregulated, and non-significant metabolites, respectively. (e) Bubble chart of KEGG pathway enrichment for differential metabolites. The x-axis indicates the enrichment factor, with larger values indicating a higher degree of gene enrichment. The size of the points corresponds to the number of metabolites, and the color reflects the *p*-value, with red indicating significant differences. (f) Total flavonoid content. *p* values are indicated as follows: *** for $p < 0.001$, ** for $p < 0.01$, and * for $p < 0.05$.

biosynthesis pathway were quantitatively analyzed. The results were calculated using $2^{-\Delta\Delta CT}$, and each value was the average of three biological replicates.

Data analysis

Data organization and analysis were performed using Excel 2021 (Microsoft Corporation Redmond WA USA). One-way analysis of

variance and T-tests were conducted using SPSS (Version 26.0 IBM Chicago IL USA) software. Statistical charts were plotted using GraphPad Prism (Version 8.0.2.263), Origin (2022), and TBtools (Version 2.029) software. The primers are shown in Supplementary Table S1.

Results

Differences in flavonoid metabolites between Huazhou pomelo and Sanhong pomelo

Analysis of total flavonoid content differences

To explore the metabolite composition of Huazhou pomelo and Sanhong pomelo, this study used ultra-high performance liquid chromatography (Vanquish UPLC) and high-resolution mass spectrometry (Q Exactive HFX) to detect metabolites in the samples. The results showed a high similarity between the Huazhou and Sanhong pomelos but significant differences between the groups. Principal component analysis (PCA) showed that the main horizontal (PC1) and vertical (PC2) axes explained 56.1% and 10.9% of the variance, respectively (Fig. 1c). A total of 1,311 metabolites were detected in both Huazhou and Sanhong pomelos, with 485 metabolites up-regulated in Sanhong pomelos, 403 down-regulated, and 423 showing no significant difference (Fig. 1d). Using a combination of *t* tests and Orthogonal Partial Least Squares-Discriminant Analysis methods, with VIP > 1 and $p < 0.05$, 150 differential metabolites were screened from 1,311 metabolites. Kyoto Encyclopedia of Genes and Genomes (KEGG) pathway enrichment analysis showed that these differential metabolites were mainly concentrated in flavonoid and flavonol biosynthesis and limonene and pinene degradation pathways (Fig. 1d). Further analysis of the flavonoid and flavonol biosynthesis pathways revealed changes in 92 genes (Supplementary Table S2). Subsequent detection of the total flavonoid content indicated that the total flavonoid concentrations of Huazhou pomelo and Sanhong pomelo were 12.0720 and 20.6200 mg/g, respectively, with the total flavonoid content of Sanhong pomelo being 1.7 times that of Huazhou pomelo (Fig. 1f).

Analysis of flavonoid compound differences

In this study, cluster analysis of 150 differential metabolites was conducted using metabolomic data to provide a more objective evaluation of the quality differences between Huazhou pomelo and Sanhong pomelo. The clustering heat map of differential metabolites visually displayed the different expression patterns of differential metabolites in Huazhou and Sanhong pomelo, with the metabolites clustered together having similar expression patterns (Fig. 2a). Among the 150 differential metabolites, nine compounds, including seven flavonoids, isoquercitrin, isorhamnetin, isovitexin, kaempferol-3-glucoside-xylose, tricin-5-glucoside, vitexin, forsythiaside, eriodictyol-7-O-neohesperidoside, and homoorientin, were selected for boxplot presentation (Fig. 3). The results showed that the relative contents of isovitexin and kaempferol-3-glucoside-xylose were higher in Huazhou pomelo than in Sanhong pomelo, and those of isoquercitrin, isorhamnetin, kaempferol-3-glucoside-xylose, wheat yellow-5-glucoside, vitexin, pinoresinol, eriodictyol-7-O-neohesperidoside, and isoorientin were higher in Sanhong pomelo than in Huazhou pomelo.

Analysis of major flavonoid compound content differences

Flavonoids, including flavone glycosides and polymethoxyflavones, are a major class of bioactive components in CGE. Based on metabolomics data, statistical analysis was performed on the relative contents of flavonoid compounds (Fig. 4). Eight flavonoid compounds, naringin, narirutin, quercetin, naringenin, isoquercitrin, rhoifolin, apigenin, and luteolin were analyzed. The relative contents of naringenin, isoquercitrin, rhoifolin, apigenin, and luteolin differed significantly between the two groups (Fig. 4). Naringenin and apigenin contents were significantly higher in Huazhou pomelo than in Sanhong pomelo, and isoquercitrin, rhoifolin, and luteolin contents were significantly higher in Sanhong pomelo than in Huazhou pomelo. Although the content of naringin, the specified detection component in the 'Chinese Pharmacopoeia', was slightly higher in Sanhong pomelo than in Huazhou pomelo, the difference was not significant.

To further understand the flavonoid content in Huazhou pomelo and Sanhong pomelo, this study selected crucial flavonoid components and determined absolute content using High Performance Liquid Chromatography (HPLC) quantitative analysis (Fig. 2b, c). The flavonoids have different absorption values at the wavelengths of 283 and 340 nm. At a wavelength of 283 nm (Fig. 2b), except for quercetin, other flavonoids, such as naringenin chalcone, naringenin, hesperidin, narirutin, diosmin, and neohesperidin, showed significant differences. At a wavelength of 340 nm (Fig. 2c), isoquercitrin, luteolin, apigenin, tangeretin, nobiletin, and rhoifolin also showed significant differences. Although the apigenin, isoquercitrin, tangeretin, and nobiletin contents were lower, these components differed significantly between the two groups and may be important flavonoids. Among the 14 flavonoids, naringin had the highest content, at 35.62 mg/g in Huazhou pomelo and 79.79 mg/g in Sanhong pomelo, followed by rhoifolin, at 7.63 and 11.29 mg/g in Huazhou pomelo and Sanhong pomelo, respectively, showing that the contents of the two components were significantly higher in Sanhong pomelo than in Huazhou pomelo. However, some flavonoids with lower contents in Sanhong pomelo but important roles, such as luteolin, apigenin, tangeretin, nobiletin, naringenin chalcone, naringenin, diosmin, and narirutin, were significantly more abundant in Huazhou pomelo.

Analysis of genes related to flavonoid synthesis

Expression levels of some flavonoid genes were higher in Huazhou pomelo than in Sanhong pomelo

A total of 3,914 differentially expressed genes were screened between Huazhou pomelo and Sanhong pomelo, with 1,892 genes up-regulated (expressed more in Sanhong pomelo than in Huazhou pomelo), 1,817 genes down-regulated (expressed more in Huazhou pomelo than in Sanhong pomelo), and 205 genes showing no change (Fig. 5a). Hierarchical clustering analysis of differentially expressed genes indicated different expression patterns of genes in Huazhou pomelo and Sanhong pomelo (Fig. 5b). KEGG enrichment analysis revealed that these differentially expressed genes were mainly enriched in pathways, such as cytochrome P450, molecular chaperones, folding catalysts, and phenylpropanoid biosynthesis (Fig. 5c).

Combined analysis of metabolomics and transcriptomics to screen flavonoid synthesis-related genes

To further explore the differences in the flavonoid synthesis pathways between Huazhou pomelo and Sanhong pomelo, a flavonoid synthesis pathway map was drawn based on the expression patterns of genes related to the phenylpropanoid and flavonoid biosynthesis pathways (Fig. 6). These genes included 31 structural genes related to flavonoid synthesis, including five phenylalanine ammonia-lyase (PAL), eight chalcone synthase (CHS), eight 4CL, two CHI, two FLS, one F3H, and five O-methyltransferase (OMT) genes. The analysis showed that 18 of these genes had higher expression levels in Huazhou pomelo than in Sanhong pomelo, particularly *PAL*, *CHI*, and *F3H*, which had higher expression levels in Huazhou pomelo than in Sanhong pomelo, whereas most CHS genes showed higher expression in Sanhong pomelo than in Huazhou pomelo.

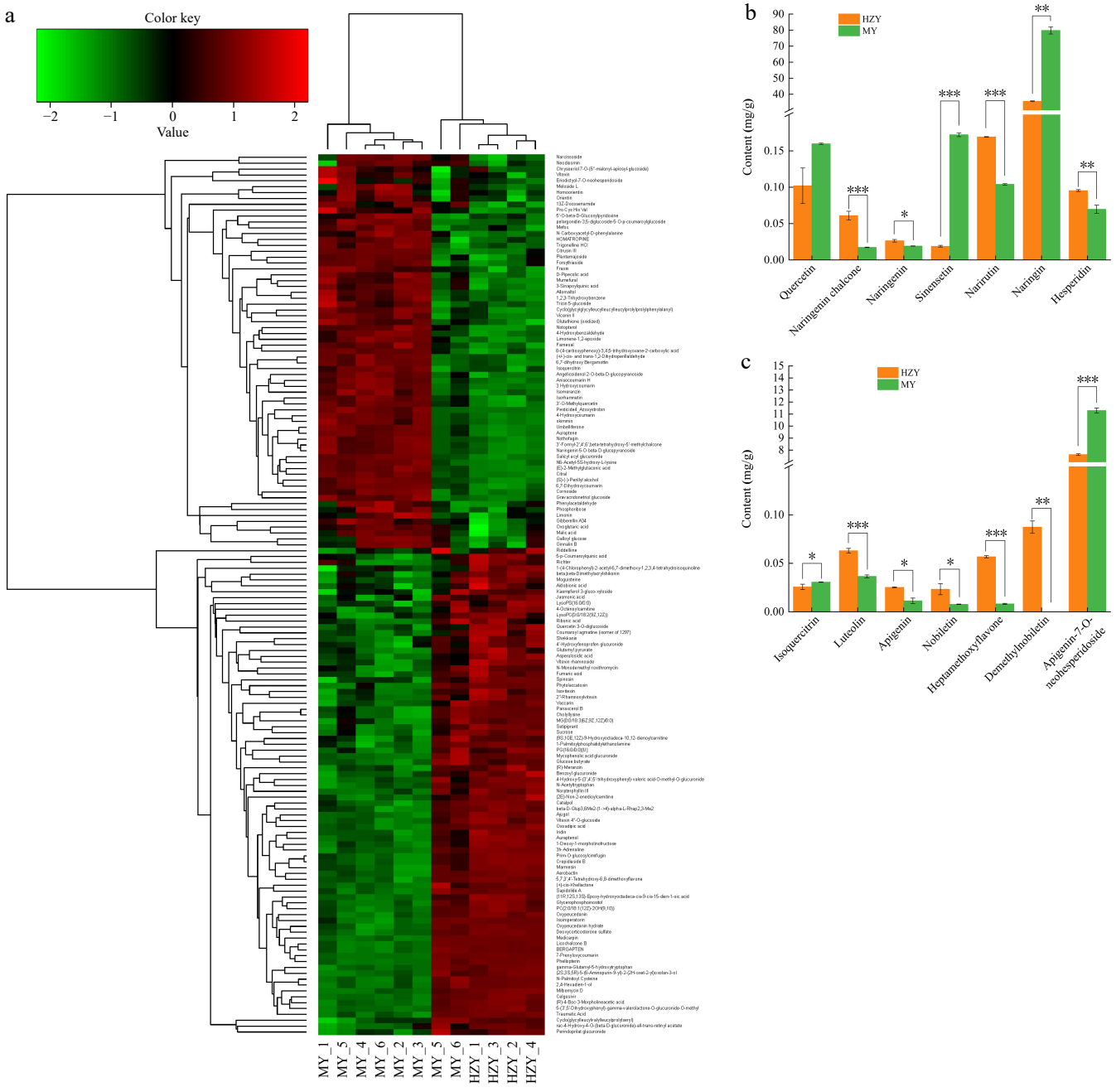

Fig. 2 Metabolomic clustering heatmap and flavonoid composition differences between Huazhou pomelo and Sanhong pomelo. (a) Hierarchical clustering heatmap of differential metabolites. The x-axis represents the samples, and the y-axis represents the differential metabolites. The color indicates the expression level, with green representing low expression and red representing high expression. (b) Content of seven flavonoid compounds at 283 nm. (c) Content of seven flavonoid compounds at 340 nm. *p* values are indicated as follows: *** for $p < 0.001$, ** for $p < 0.01$, and * for $p < 0.05$.

Additionally, heat maps of the contents related to luteolin, apigenin, rhoifolin, naringenin chalcone, naringenin, quercetin, narirutin, diosmin, and isoquercitrin were drawn.

To increase the accuracy of the screen for key genes affecting flavonoid synthesis in CGE, this study used a combined metabolomics and transcriptomics analysis. After removing low-expression genes, weighted gene co-expression network analysis (WGCNA) was conducted on 14,844 genes obtained from the transcriptome, resulting in 28 different gene modules (Fig. 7b). Correlation analysis was performed between the absolute contents of the 13 flavonoids detected by HPLC and the gene modules obtained by WGCNA, revealing significant correlations between flavonoid content and certain gene modules with similar expression patterns (Fig. 7c). Further analysis combined with the heat map of key flavonoid content (Fig. 7a) showed that the second group of flavonoid components, such as diosmin, luteolin, naringenin chalcone, narirutin, tangeretin, apigenin, naringenin, and nobiletin, had a higher content in Huazhou pomelo than in Sanhong pomelo, whereas another group of flavonoid components, including rhoifolin, hesperidin, naringin, quercetin, and isoquercitrin, had a higher content in Sanhong pomelo than in Huazhou pomelo (Fig. 7c).

As shown in Fig. 7c, the second group of flavonoids was primarily concentrated in the right half. Based on the correlation between the second group of flavonoid components and the 28 identified modules, the brown module (MEbrown) stands out as a prominent module, with its genes potentially associated with flavonoid

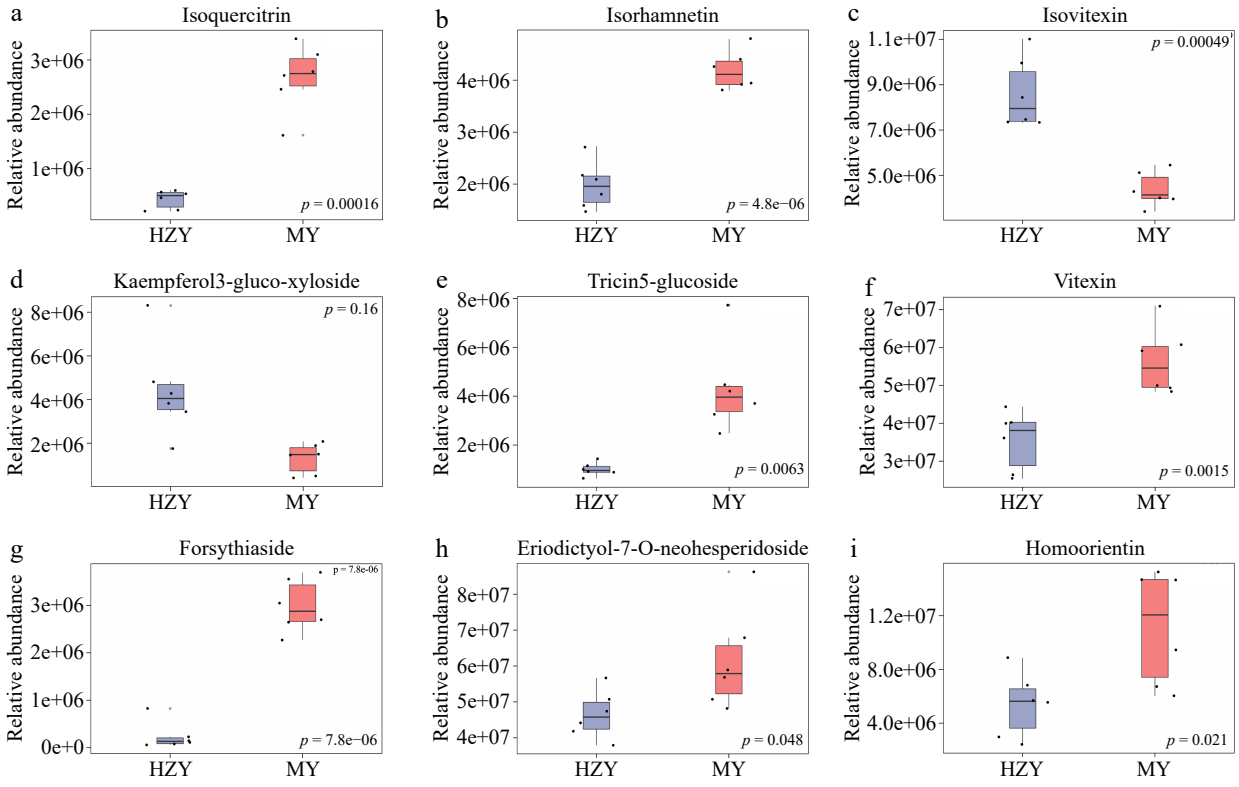

Fig. 3 Boxplots of selected differential metabolites. (a) Isoquercitrin, (b) isorhamnetin, (c) isovitexin, (d) kaempferol-3-glucoside-xylose, (e) tricin-5-glucoside, (f) vitexin, (g) forsythiaside, (h) eriodictyol-7-O-neohesperidoside, and (i) homoorientin. Note: The x-axis represents the groups, with each bar representing one group. The y-axis represents the relative abundance of metabolites. Each boxplot corresponds to five statistical measures, from top to bottom: maximum, upper quartile, median, lower quartile, and minimum.

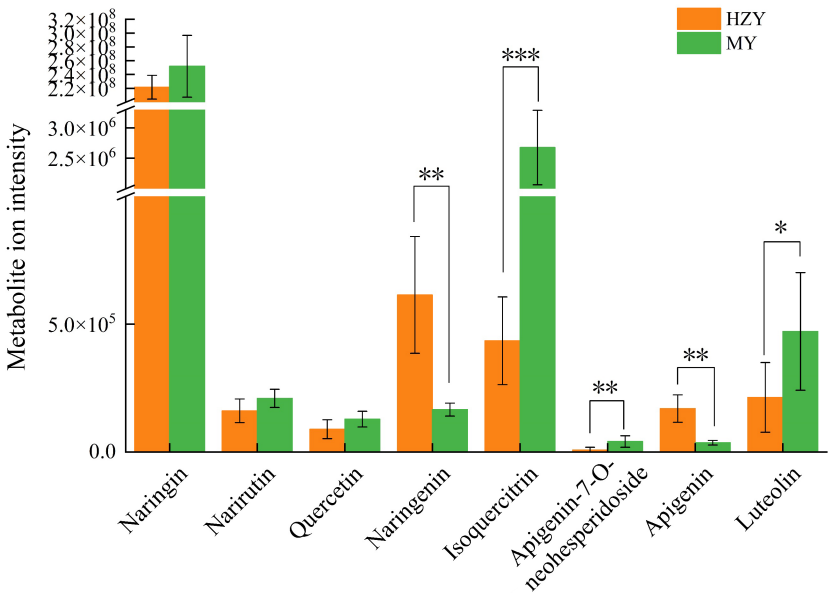

Fig. 4 Metabolite ion intensity plots for metabolites involved in flavonoid biosynthesis in Huazhou and Sanhong pomelo. High average ion intensity indicates that the metabolite has a higher abundance or concentration in the sample. Low average ion intensity indicates that the metabolite has a lower abundance or concentration in the sample. *p*-values are indicated as follows: *** for $p < 0.001$, ** for $p < 0.01$, and * for $p < 0.05$.

metabolic pathways, exhibiting high correlations: nobiletin (r = 0.9, $p = 0.002$), hesperetin (r = 0.9, $p = 0.002$), hesperetin chalcone (r = 0.82, $p = 0.01$), heptamethoxyflavone (r = 0.79, $p = 0.02$), narirutin (r = 0.78, $p = 0.02$), quercetin (r = −0.8, $p = 0.02$), naringin (r = −0.78, $p = 0.02$), sinensetin (r = −0.78, $p = 0.02$), and farrerol (r = −0.77, $p = 0.02$). Subsequently, genes with a module correlation value greater than 0.8 and gene significance greater than 0.8 were selected, resulting in the identification of 231 hub genes from a total of 1,301 genes in the brown module.

As shown in Figs 6 and 7a, the higher hesperetin chalcone content in Huazhou pomelo than in Sanhong pomelo may be related to the genes *CgPAL1*, *CgPAL2*, *CgPAL3*, *CgPAL4*, *CgPAL5*,

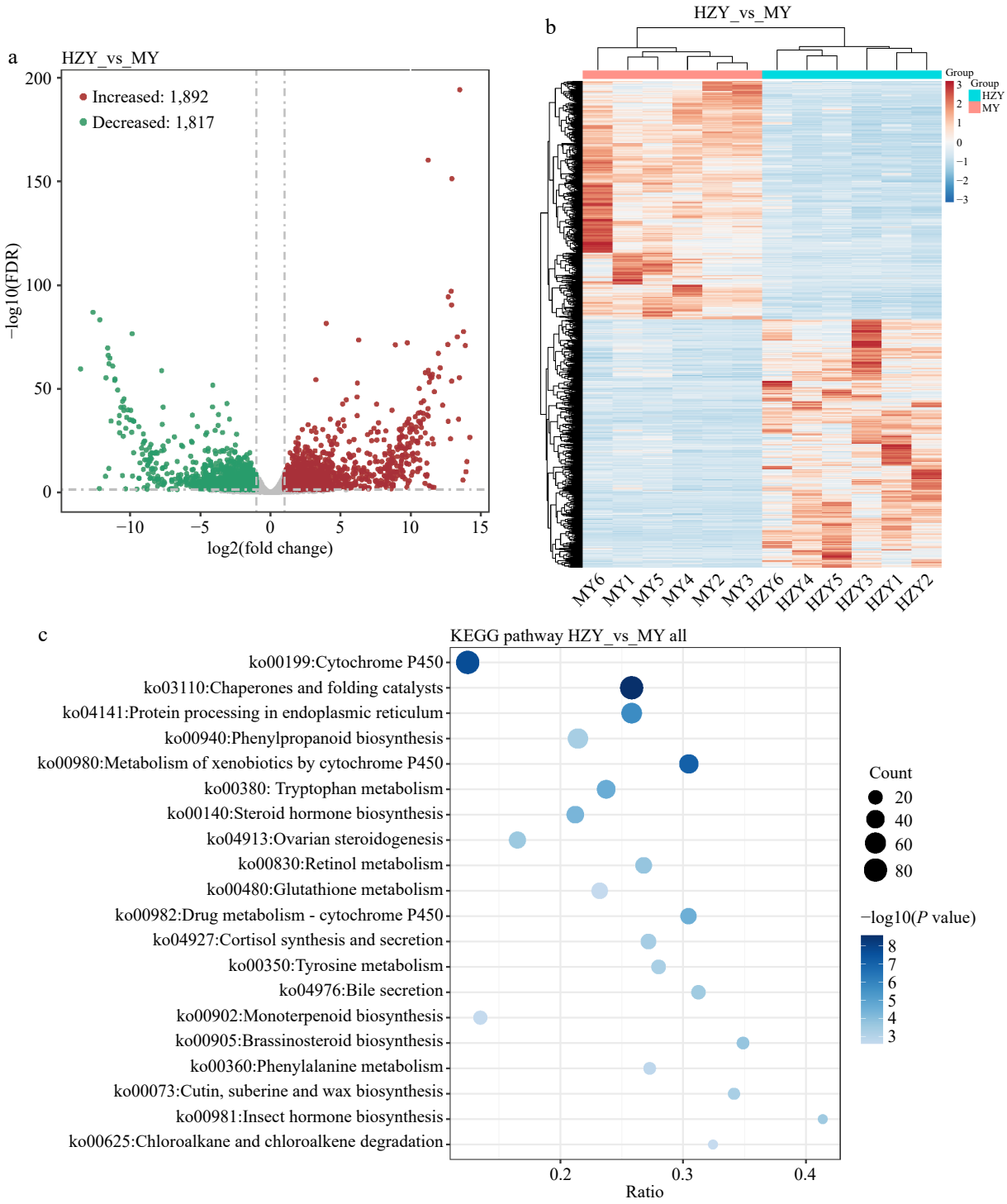

Fig. 5 Transcriptomic results of Huazhou pomelo and Sanhong pomelo. (a) Volcano plot of differentially expressed genes. The x-axis represents the logarithmic value of the fold change in gene expression (log2 fold change), and the y-axis represents the negative logarithmic value of the FDR (false discovery rate). Each point represents a gene, with red points indicating upregulated genes, green points indicating downregulated genes, and gray points indicating non-significant genes. (b) Hierarchical clustering heatmap of differentially expressed genes. Columns represent different samples, and rows represent different genes. Red and blue indicate high and low gene expression in the samples, respectively. (c) Bubble chart of KEGG pathway enrichment analysis for differentially expressed genes. The x-axis represents the ratio of differentially expressed genes enriched in the pathway to the total number of genes enriched in the pathway. Larger values indicate a higher degree of enrichment of differentially expressed genes in the KEGG pathway.

Cg4CL1, *Cg4CL2*, *Cg4CL4*, *Cg4CL5*, *Cg4CL6*, *CgCHS2*, *CgCHS4*, and *CgCHS5*. The higher hesperetin content in Huazhou pomelo than in Sanhong pomelo may be associated with the aforementioned genes and *CgCHI1* and *CgCHI2*. Conversely, the lower quercetin content in Huazhou pomelo than in Sanhong pomelo may be linked to *CgFLS2*, *CgOMT1*, and *CgOMT5*.

Therefore, among the aforementioned structural genes potentially associated with flavonoid content in Huazhou pomelo, this

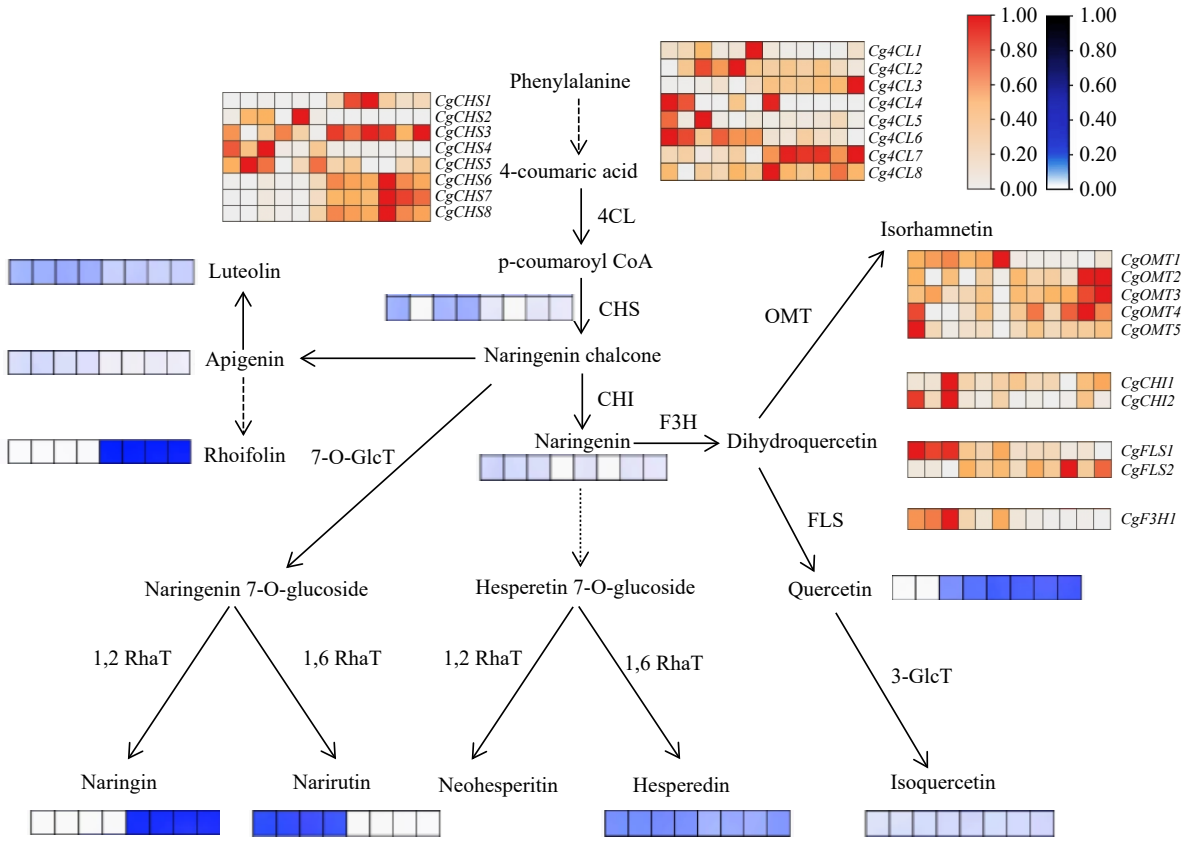

Fig. 6 Flavonoid biosynthesis pathway in Huazhou pomelo. In the heatmap, the samples are arranged from left to right as H1, H2, H3, H4, H5, H6, M1, M2, M3, M4, M5, and M6. Gene expression levels are represented by FPKM values obtained from transcriptome sequencing, with colors ranging from white to red to indicate low to high FPKM values. Additionally, heatmaps depicting the content of certain flavonoid monomers, determined via HPLC, are illustrated around the pathway. Here, colors range from white to blue to represent low to high flavonoid content. The samples for these heatmaps are arranged from left to right as H1, H2, H3, H4, M1, M2, M3, and M4.

study excluded genes with low expression levels, resulting in selecting *CgPAL1*, *CgPAL2*, *CgPAL5*, *Cg4CL1*, *Cg4CL2*, *CgCHS4*, *CgCHI2*, and *CgOMT1* for correlation analysis with the previously identified 231 hub genes. Genes with correlations ≤ |0.6| were filtered out and the results are shown in Fig. 7d. These key structural genes, including *CgCHS4*, *CgPAL2*, *CgOMT1*, *CgPAL5*, *Cg4CL1*, and *CgCHI2*, may be positively correlated with *Cg1150p95.2*, *Cg0510p7.2*, *Cg0710p43.3*, *Cg0070a116.19*, *Cg0330s24.80*, and *Cg1670s42.49* and negatively correlated with *Cg1290s11.25* and *Cg1300s1.31* (Fig. 7d, red arrows). These genes may represent the major differential genes between Huazhou pomelo and Sanhong pomelo.

Based on the genes shown in Fig. 6, 11 key genes associated with flavonoid biosynthesis pathways that showed significant differential expression in the transcriptome were further screened. Their expression levels in Huazhou pomelo and Sanhong pomelo were analyzed using qRT-PCR (Fig. 8). These genes, including *CgPAL2* (Cg0070a91.31), *CgPAL8* (Cg1290a64.43), *Cg4CL2* (Cg0540p8.5), *Cg4CL6* (Cg0550a31.21), *CgCHI2* (Cg1290p88.2), *CgF3H1* (Cg0650p13.4), *CgFLS*1 (Cg0910s46.62), *CgOMT1* (Cg0330p53.1), *CgOMT3* (Cg1430s9.10), and *CgOMT5* (Cg0150a89.16), exhibited higher expression levels in Huazhou pomelo than in Sanhong pomelo, with the former showing fold changes of 0.70, 1.73, 2.36, 2.85, 0.15, 3.96, 2.01, 11.50, 2.76, and 2.60, respectively. Additionally, *CgCHS4* (Cg1300s23.17) showed higher expression in Sanhong pomelo than in Huazhou pomelo, with the former having a 14.25-fold increase.

Discussion

This study systematically compared the main flavonoid components and differences in their synthesis-related genes between Huazhou pomelo and Sanhong pomelo using metabolomic and transcriptomic methods. The results showed that although the total flavonoid content differed significantly between the two pomelos, both contained most of the flavonoid components found in CGE. Huazhou pomelo had a clear advantage in the content of certain key flavonoid components, which may be one of the main reasons for its use as an authentic medicinal material.

The total flavonoid content differed significantly between Huazhou pomelo and Sanhong pomelo. Although the content of naringin, a specified detection component in the 'Chinese Pharmacopoeia', was slightly higher in Sanhong pomelo than in Huazhou pomelo, the difference was not significant. However, the contents of naringenin, apigenin, tangeretin, nobiletin, and rhoifolin in Huazhou pomelo were significantly higher than those in Sanhong pomelo, especially nobiletin, which was only present in Huazhou pomelo. These components exhibit significant bioactivity, including antioxidant, anti-inflammatory, anticancer, and antiviral properties[30–33]. For example, naringenin has been widely studied and demonstrated to have anti-inflammatory, cough-relieving, and phlegm-resolving effects and significantly inhibit various inflammatory factors[34–38]. Apigenin is a multifunctional flavonoid with antioxidant, anticancer, neuroprotective, antiviral, anti-inflammatory, and cardiovascular protective properties[39–44]. Studies have shown that

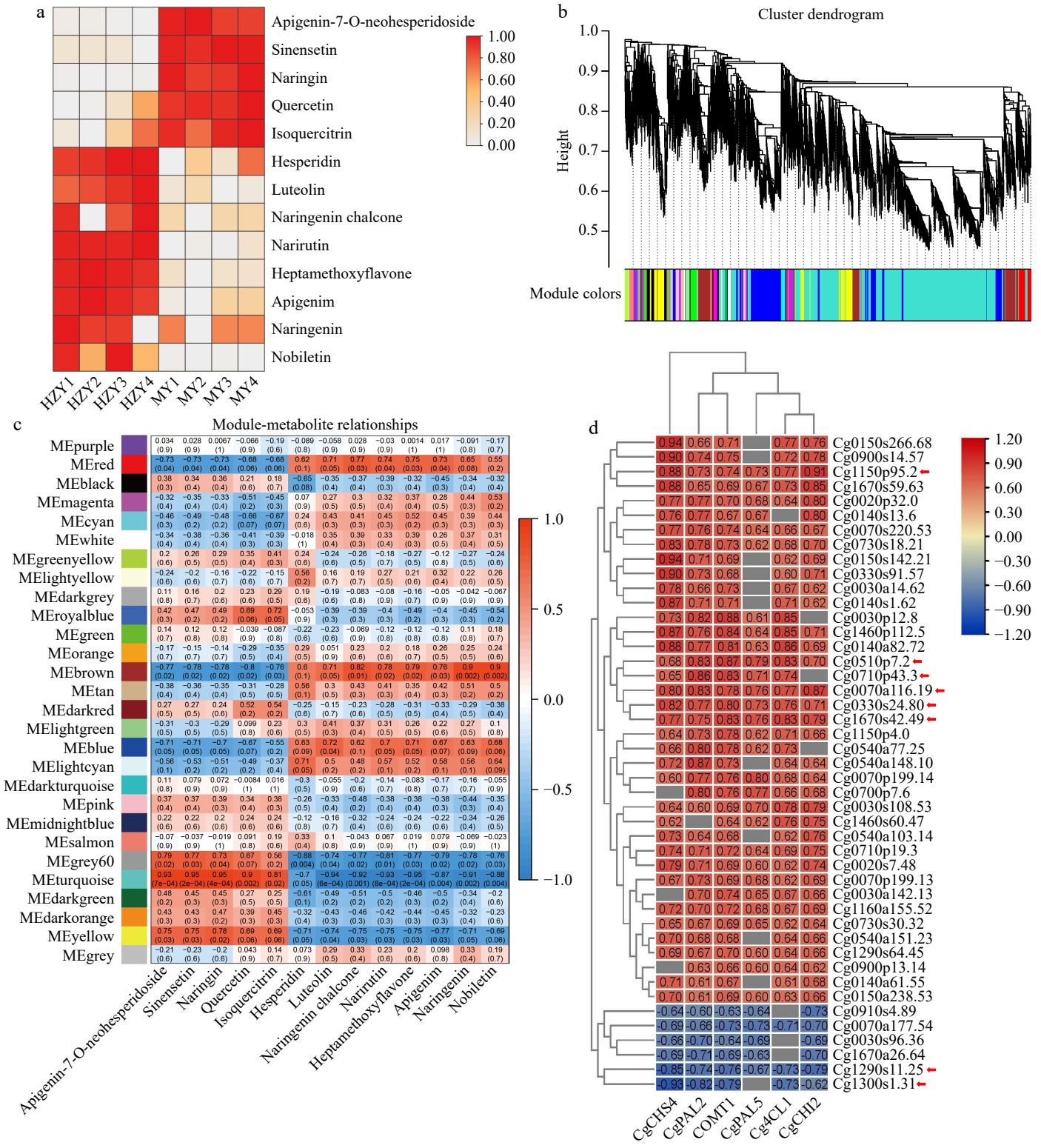

Fig. 7 Integrated analysis of metabolome and transcriptome. (a) Heatmap of the content of selected flavonoid monomers, with colors ranging from white to red indicating low to high flavonoid content. H1-4 represent Huazhou pemelo, and M1-4 represent Sanhong pomelo. (b) Hierarchical clustering dendrogram, showing 28 co-expression gene modules identified by WGCNA. (c) Correlation between flavonoids and WGCNA modules. The axes represent the 28 modules obtained from WGCNA and the different types of flavonoids, respectively. Each intersection in the grid shows the Pearson correlation coefficient and *p*-value for the module and flavonoid. The Pearson coefficient with large correlation indicates the strong correlation of the corresponding module with flavonoids. (d) Correlation analysis between important structural genes and genes. The x-axis represents the different structural genes, while the y-axis represents the hub genes. Each intersection in the grid displays the correlation coefficient values between the structural genes and hub genes.

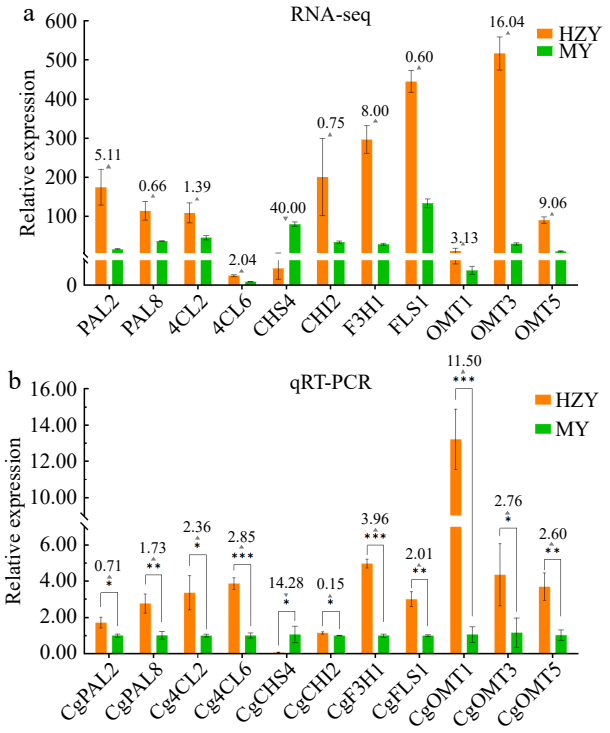

Fig. 8 Expression pattern of 11 key flavonoid biosynthesis genes in Huazhou and Sanhong pomelo. (a) Transcriptomic analysis of the expression pattern of 11 key genes in the flavonoid biosynthesis pathway. (b) Expression patterns of 11 key genes flavonoid biosynthesis pathway determined by qRT-PCR. Note: Upward triangles indicate the fold increase in relative gene expression of Huazhou pomelo (HZY) compared to Sanhong pomelo (MY). Downward triangles indicate the fold decrease in relative gene expression of Huazhou pomelo (HZY) compared to Sanhong pomelo (MY).

apigenin exerts its anticancer effects by regulating multiple signaling pathways, such as PI3K/Akt, MAPK, and NF-κB[42].

Tangeretin and nobiletin are another class of important polymethoxyflavones (PMFs), and the contents of these components were significantly higher in Huazhou pomelo than in Sanhong pomelo. Tangeretin has strong anti-inflammatory, anticancer, antioxidant, and antiviral activities with significant inhibitory effects on inflammation and cancer growth[45–47]. Nobiletin has shown strong anticancer activity in various cancer models, with mechanisms including induction of apoptosis, inhibition of cell proliferation, and inhibition of cancer cell invasion[10,48–50]. Nobiletin, which was present in Huazhou pomelo but not Sanhong pomelo, has significant anti-inflammatory and anticancer activities; however, its specific mechanism requires further research[30–33]. In this study, certain flavonoids with relatively low concentrations but significant functional roles were notably higher in Huazhou pomelo than in Sanhong pomelo. These flavonoids were hesperetin, apigenin, hesperidin, and polymethoxyflavones (e.g., demethylnobiletin, nobiletin, heptamethoxyflavone, hesperetin chalcone). These results indicate that the Huazhou pomelo, as a key source of CGE, possesses a superior material foundation to the Sanhong pomelo.

Flavonoids are synthesized from phenylalanine via the phenylpropanoid pathway, and phenylalanine is produced via the shikimate pathway[51]. The key enzymes in this process include PAL, cinnamate-4-hydroxylase (C4H), and 4-coumaroyl-CoA ligase (4CL), which together catalyze the conversion of phenylalanine to p-coumaroyl-CoA[52–54]. Subsequently, p-coumaroyl-CoA is converted into flavanones (e.g., naringenin) via catalysis by CHS and isomerase (CHI). Naringenin, a critical precursor of multiple subclasses of the flavonoid family, is further synthesized into different flavonoid compounds (e.g., flavones, flavanols, anthocyanins, proanthocyanidins, isoflavones) through various pathways[55].

PAL, a rate-limiting enzyme in the phenylalanine metabolic pathway, plays a critical role in the synthesis of precursors such as flavonoids and phenolic acids, and in regulating carbon flux from primary to secondary metabolism[56–57]. For instance, in strawberry fruits, PAL activity is closely correlated with the concentration of anthocyanins and other phenolic compounds[58]. Furthermore, studies on chrysanthemum have indicated that *CmPAL1* and *CmPAL2* are involved in flavonoid compounds[59]. The *4CL* gene family exhibits diversity in plant metabolism owing to substrate specificity among its members. In Arabidopsis, *At4CL3* plays a significant role in flavonoid metabolism, and its activity is positively correlated with flavonol content[60,61]. CHS and CHI are the first and second most important rate-limiting enzymes involved in flavonoid biosynthesis, respectively[62,63]. CHS, through its polyketide synthase function, plays a decisive role in regulating total flavonoid content[64]. Similarly, CHI expression levels are significantly associated with flavonoid content in Arabidopsis[65]. Overexpression of *DcCHI1* or *DcCHI4* in tobacco was shown to significantly enhance flavonoid accumulation[66]. Research on buckwheat confirmed that CHS and CHI are essential for anthocyanin accumulation[67]. This study suggests that the higher levels of hesperetin chalcone, hesperetin, hesperidin, and narirutin in Huazhou pomelo than in Sanhong pomelo may be associated with the expression of *CgPAL*, *Cg4CL*, *CgCHS*, and *CgCHI*.

PMFs, including sinensetin, quercetin, nobiletin, and tangeretin, are a unique class of flavonoids that contain multiple methoxy (-OCH3) groups, including sinensetin, quercetin, nobiletin, and tangeretin[68–70]. PMFs are abundant in the peel of citrus fruits and exhibit various biological activities, such as anticancer, anti-inflammatory, and antiviral properties[46,47]. Among PMFs, nobiletin demonstrates strong biological activities, including suppressing inflammation and cancer growth and preventing metabolic syndrome and cardiovascular diseases[5,47,71]. Naringenin, as a core precursor in PMF biosynthesis, is regulated by CHS and CHI[21]. Early flavonoid biosynthesis genes (e.g., CHS and CHI) contribute to naringenin production, and late biosynthesis genes such as FLS and F3H modify naringenin to generate various naringenin derivatives[21]. Furthermore, flavonoid OMT is a key enzyme in the PMF biosynthesis pathway and is responsible for the methylation of O-flavonoid aglycones, which influence PMF accumulation[1,21,72].

The expression of *CreOMT3*, *CreOMT4*, and *CreOMT5* is closely related to the accumulation of six PMF monomers and total PMFs in six *Citrus reticulata* varieties. Particularly, the expression of *CreOMT1* was significantly associated with nobiletin accumulation[73]. In *C. reticulata* 'Chachiensis', *CcOMT1* exhibits relatively high and stable gene expression throughout development, making it a candidate enzyme for PMF biosynthesis; additionally, multi-omics studies identified a novel OMT gene, *CtgOMT1*, in Huazhou pomelo and proposed its involvement in nobiletin synthesis. Similarly, in *C. reticulata*, a *CsCCoAOMT1* gene has been identified, which is involved in the synthesis of six major PMFs and significantly promotes the accumulation of nobiletin and heptamethoxyflavone[1,21,74]. This study indicated that *CgCHI2* (Cg1290p88.2), *CgF3H1* (Cg0650p13.4), *CgFLS1* (Cg0910s46.62), *CgOMT1* (Cg0330p53.1), *CgOMT3* (Cg1430s9.10), and *CgOMT5* (Cg0150a89.16) were highly expressed in Huazhou pomelo, which might explain the higher levels of polymethoxyflavones, such as demethylnobiletin, nobiletin, and heptamethoxyflavone, in Huazhou pomelo fruit than in Sanhong pomelo.

In summary, genes such as *CgPAL*, *CgCHS*, *CgCHI*, *CgFLS*, and *CgOMT* may influence flavonoid accumulation in Huazhou pomelo, particularly the accumulation of key flavonoids at high concentrations. However, the specific functions of these genes require further research. Moreover, among the eight genes related to these structural genes in Huazhou pomelo, six were positively correlated, and two were negatively correlated with flavonoid synthesis. However, their precise function requires further investigation.

Overall, as an authentic medicinal material for CGE, Huazhou pomelo has significant advantages in the context of key flavonoid components and the expression of synthesis-related genes. These advantages not only demonstrate that the quality of Huazhou pomelo is superior to that of Sanhong pomelo but also provide scientific evidence for the quality control and authenticity evaluation of CGE. Due to constraints on research design, methodology, or factors that affect the findings, further studies are needed.

Conclusions

In conclusion, Huazhou pomelo has a significant advantage in the accumulation and synthesis of flavonoid compounds, which scientifically validate its status as an authentic medicinal material for CGE. However, Sanhong pomelo contained the most flavonoid components, particularly naringin, a key component specified by the Chinese Pharmacopoeia, which was higher in Sanhong pomelo than in Huazhou pomelo. Therefore, the results have demonstrated that pomelo (honey pomelo) can be used as a source of CGE; however, separate quality standards should be established for Huazhou pomelo and other pomelos. We recommend the inclusion of content detection indicators for nobiletin, tangeretin, and nobiletin in the formulation of quality standards for CGE, which should be sourced from Huazhou pomelo, to ensure high quality and promote its sustainable development in the traditional Chinese medicine industry.

Author contributions

The authors confirm contribution to the paper as follows: study conception and design: Wu H; experiments design: Wu H, Bai M; experiments performed and the data analysis: Huang H, Liu Y, Su J, Liang X; draft manuscript preparation: Bai M, Huang H, Wu H. All authors reviewed the results and approved the final version of the manuscript.

Data availability

All data associated with this paper are provided within the figures and supplementary data published online.

Acknowledgments

This work was supported by The Open Competition Program of Ten Major Directions of Agricultural Science and Technology Innovation for the 14th Five-Year Plan of Guangdong Province (No. 2022SDZG07 to H.W.), the National Natural Science Foundation of China (No. 32270381 to M.B.), and the Natural Science Foundation of Guangdong (No. 2022A1515011086 to M.B.).

Conflict of interest

Authors declare that they have no competing interests. Dr. Hong Wu is the Editorial Board member of *Medicinal Plant Biology* who was blinded from reviewing or making decisions on the manuscript. The article was subject to the journal's standard procedures, with peer-review handled independently of this Editorial Board member and the research groups.

Supplementary information accompanies this paper at (https://www.maxapress.com/article/doi/10.48130/mpb-0024-0033)

Dates

Received 11 November 2024; Revised 18 December 2024; Accepted 23 December 2024; Published online 4 March 2025

References

1. Xian L, Sahu SK, Huang L, Fan Y, Lin J, et al. 2022. The draft genome and multi-omics analyses reveal new insights into geo-herbalism properties of *Citrus grandis* 'Tomentosa'. *Plant Science* 325:111489
2. Li PL, Liu MH, Hu JH, Su WW. 2014. Systematic chemical profiling of *Citrus grandis* 'Tomentosa' by ultra-fast liquid chromatography/diode-array detector/quadrupole time-of-flight tandem mass spectrometry. *Journal of Pharmaceutical and Biomedical Analysis* 90:167–79
3. Fan R, Zhu C, Qiu D, Zeng J. 2019. Comparison of the bioactive chemical components and antioxidant activities in three tissues of six varieties of *Citrus grandis* 'Tomentosa' fruits. *International Journal of Food Properties* 22(1):1848–62
4. Huang X, Liu X, Wang Q, Zhou Y, Deng S, et al. 2024. Transcriptomic and targeted metabolome analyses revealed the regulatory mechanisms of the synthesis of bioactive compounds in *Citrus grandis* 'Tomentosa'. *Peer J* 12:e16881
5. Rong N, Huang L, Ye P, Pan H, Hu M, et al. 2024. CgLS mediates limonene synthesis of main essential oil component in secretory cavity cells of *Citrus grandis* 'Tomentosa' fruits. *International Journal of Biological Macromolecules* 280:135671
6. Jiang K, Song Q, Wang L, Xie T, Wu X, et al. 2014. Antitussive, expectorant and anti-inflammatory activities of different extracts from Exocarpium *Citri grandis*. *Journal of Ethnopharmacology* 156:97–101
7. Jiao HY, Su WW, Li PB, Liao Y, Zhou Q, et al. 2015. Therapeutic effects of naringin in a guinea pig model of ovalbumin-induced cough-variant asthma. *Pulmonary Pharmacology & Therapeutics* 33:59–65
8. Ang L, Lee HW, Choi JY, Zhang J, Lee MS. 2020. Herbal medicine and pattern identification for treating COVID-19: a rapid review of guidelines. *Integrative Medicine Research* 9(2):100407
9. Su W, Wang Y, Li P, Wu H, Zeng X, et al. 2020. The potential application of the traditional Chinese herb *Exocarpium Citri grandis* in the prevention and treatment of COVID-19. *Traditional Medicine Research* 5:160–66
10. Jang SE, Ryu KR, Park SH, Chung S, Teruya Y, et al. 2013. Nobiletin and tangeretin ameliorate scratching behavior in mice by inhibiting the action of histamine and the activation of NF-κb, AP-1 and P38. *International Immunopharmacology* 17(3):502–7
11. Peng Y, Hu M, Lu Q, Tian Y, He W, et al. 2019. Flavonoids derived from *Exocarpium Citri Grandis* inhibit LPS-induced inflammatory response via suppressing MAPK and NF-κB signalling pathways. *Food and Agricultural Immunology* 30(1):564–80
12. Fang J, Cao Z, Song X, Zhang X, Mai B, et al. 2020. Rhoifolin alleviates inflammation of acute inflammation animal models and LPS-induced RAW264.7 cells via IKKβ/NF-κB signaling pathway. *Inflammation* 43(6):2191–210
13. Duan L, Guo L, Dou LL, Yu KY, Liu EH, et al. 2014. Comparison of chemical profiling and antioxidant activities of fruits, leaves, branches, and flowers of *Citrus grandis* 'Tomentosa'. *Journal of Agricultural and Food Chemistry* 62(46):11122–29
14. Zhang M, Nan H, Wang Y, Jiang X, Li Z. 2014. Comparison of flavonoid compounds in the flavedo and juice of two pummelo cultivars (*Citrus grandis* (L.) Osbeck) from different cultivation regions in China. *Molecules* 19(11):17314–28
15. Ou MC, Liu YH, Sun YW, Chan CF. 2015. The composition, antioxidant and antibacterial activities of cold-pressed and distilled essential oils of *Citrus paradisi* and *Citrus grandis* (L.) Osbeck. *Evidence-based Complementary and Alternative Medicine: eCAM* 2015:804091
16. Wang F, Chen L, Chen H, Chen S, Liu Y. 2019. Analysis of flavonoid metabolites in citrus peels (*Citrus reticulata* "Dahongpao") using UPLC-ESI-MS/MS. *Molecules* 24(15):2680

17. Guo L, Yao H, Chen W, Wang X, Ye P, et al. 2022. Natural products of medicinal plants: biosynthesis and bioengineering in post-genomic era. *Horticulture Research* 9:uhac223
18. Su J, Wang Y, Bai M, Peng T, Li H, et al. 2023. Soil conditions and the plant microbiome boost the accumulation of monoterpenes in the fruit of *Citrus reticulata* 'Chachi'. *Microbiome* 11:61
19. Wen J, Wang Y, Lu X, Pan H, Jin D, et al. 2024. An integrated multi-omics approach reveals polymethoxylated flavonoid biosynthesis in *Citrus reticulata* cv. Chachiensis. *Nature Communications* 15:3991
20. Yu F, Xu X, Lin S, Peng T, Zeng . 2022. Integrated metabolomics and transcriptomics reveal flavonoids glycosylation difference in two *Citrus* peels. *Scientia Horticulturae* 292:110623
21. Fan R, Zhu C, Qiu D, Mao G, Mueller-Roeber B, et al. 2023. Integrated transcriptomic and metabolomic analyses reveal key genes controlling flavonoid biosynthesis in *Citrus grandis* 'Tomentosa' fruits. *Plant Physiology and Biochemistry* 196:210–21
22. Fan R, Qiu D, Mao G, Zeng J. 2024. Combined analysis of GC-MS, RNA-seq and ATAC-seq elucidates the essential oils variation and terpenes biosynthesis in *Citrus grandis* 'Tomentosa'. *Industrial Crops and Products* 209:117996
23. Wan H, Liu Y, Wang T, Jiang P, Wen W, et al. 2023. Combined transcriptomic and metabolomic analyses identifies *CsERF003*, a citrus ERF transcription factor, as flavonoid activator. *Plant Science* 334:111762
24. Zheng W, Zhang W, Liu D, Yin M, Wang X, et al. 2023. Evolution-guided multiomics provide insights into the strengthening of bioactive flavone biosynthesis in medicinal pummelo. *Plant Biotechnology Journal* 21(8):1577–89
25. Chen S, Zhou Y, Chen Y, Gu J. 2018. fastp: an ultra-fast all-in-one FASTQ preprocessor. *Bioinformatics* 34(17):i884–i890
26. Kim D, Paggi JM, Park C, Bennett C, Salzberg SL. 2019. Graph-based genome alignment and genotyping with HISAT2 and HISAT genotype. *Nature Biotechnology* 37(8):907–15
27. Kovaka S, Zimin AV, Pertea GM, Razaghi R, Salzberg SL, et al. 2019. Transcriptome assembly from long-read RNA-seq alignments with StringTie2. *Genome Biology* 20(1):1–13
28. Anders S, Huber W. 2010. Differential expression analysis for sequence count data. *Genome Biology* 11(10):R106
29. Langfelder P, Horvath S. 2008. WGCNA: an R package for weighted correlation network analysis. *BMC Bioinformatics* 9(1):559
30. Xu JJ, Wu X, Li MM, Li GQ, Yang YT, et al. 2014. Antiviral activity of polymethoxylated flavones from "Guangchenpi", the edible and medicinal pericarps of *Citrus reticulata* 'chachi'. *Journal of Agricultural and Food Chemistry* 62(10):2182–89
31. Benavente-García O, Castillo J. 2008. Update on uses and properties of citrus flavonoids: new findings in anticancer, cardiovascular, and anti-inflammatory activity. *Journal of Agricultural and Food Chemistry* 56(15):6185–6205
32. Saito T, Abe D, Nogata Y. 2015. Polymethoxylated flavones potentiate the cytolytic activity of NK leukemia cell line KHYG-1 via enhanced expression of granzyme B. *Biochemical and Biophysical Research Communications* 456(3):799–803
33. Guo J, Tao H, Cao Y, Ho CT, Jin S, et al. 2016. Prevention of obesity and type 2 diabetes with aged *Citrus* peel (Chenpi) extract. *Journal of Agricultural and Food Chemistry* 64(10):2053–61
34. Gao S, Li P, Yang H, Fang S, Su W. 2011. Antitussive effect of naringin on experimentally induced cough in guinea pigs. *Planta Medica* 77(1):16–21
35. Luo YL, Zhang CC, Li PB, Nie YC, Wu H, et al. 2012. Naringin attenuates enhanced cough, airway hyperresponsiveness and airway inflammation in a guinea pig model of chronic bronchitis induced by cigarette smoke. *International Immunopharmacology* 13(3):301–7
36. Lin BQ, Li PB, Wang YG, Peng W, Wu Z, et al. 2008. The expectorant activity of naringenin. *Pulmonary Pharmacology & Therapeutics* 21(2):259–63
37. Nie YC, Wu H, Li PB, Xie LM, Luo YL, et al. 2012. Naringin attenuates EGF-induced MUC5AC secretion in A549 cells by suppressing the cooperative activities of MAPKs-AP-1 and IKKs-IκB-NF-κB signaling pathways. *European Journal of Pharmacology* 690(1-3):207–13
38. Chen Y, Wu H, Nie YC, Li PB, Shen JG, et al. 2014. Mucoactive effects of naringin in lipopolysaccharide-induced acute lung injury mice and beagle dogs. *Environmental Toxicology and Pharmacology* 38(1):279–87
39. Jumah Masoud Mohammad S, Zhang XP, Joe Antony J, Chen BA. 2017. Apigenin's anticancer properties and molecular mechanisms of action: Recent advances and future prospectives. *Chinese Journal of Natural Medicines* 15(5):321–29
40. Nabavi SF, Khan H, D'Onofrio G, Dunja Š, Shirooie S, et al. 2018. Apigenin as neuroprotective agent: Of mice and men. *Pharmacological Research* 128:359–65
41. Osonga FJ, Akgul A, Miller RM, Eshun GB, Yazgan I, et al. 2019. Antimicrobial activity of a new class of phosphorylated and modified flavonoids. *ACS Omega* 4(7):12865–71
42. Chen P, Huo X, Liu W, Li K, Sun Z, et al. 2020. Apigenin exhibits anti-inflammatory effects in LPS-stimulated BV2 microglia through activating GSK3β/Nrf2 signaling pathway. *Immunopharmacology and Immunotoxicology* 42(1):9–16
43. Kashyap P, Shikha D, Thakur M, Aneja A. 2021. Functionality of apigenin as a potent antioxidant with emphasis on bioavailability, metabolism, action mechanism and *in vitro* and *in vivo* studies: a review. *Journal of food biochemistry* 46(4):e13950
44. Thomas SD, Jha NK, Jha SK, Sadek B, Ojha S. 2023. Pharmacological and molecular insight on the cardioprotective role of apigenin. *Nutrients* 15(2):385
45. Shi MD, Liao YC, Shih YW, Tsai LY. 2013. Nobiletin attenuates metastasis via both ERK and PI3K/Akt pathways in HGF-treated liver cancer HepG2 cells. *Phytomedicine* 20(8-9):743–52
46. Li S, Wang H, Guo L, Zhao H, Ho CT. 2014. Chemistry and bioactivity of nobiletin and its metabolites. *Journal of Functional Foods* 6:2–10
47. Rong X, Xu J, Jiang Y, Li F, Chen Y, et al. 2021. Citrus peel flavonoid nobiletin alleviates lipopolysaccharide-induced inflammation by activating IL-6/STAT3/FOXO3a-mediated autophagy. *Food & function* 12(3):1305–17
48. Sunagawa Y, Funamoto M, Suzuki A, Shimizu K, Sakurai R, et al. 2017. A novel target molecule of nobiletin derived from *Citrus* peels has a therapeutic potency against the development of heart failure. *European cardiology* 12(2):105
49. Zhang X, Han L, Liu J, Xu Q, Guo Y, et al. 2018. Pharmacokinetic study of 7 compounds following oral administration of fructus aurantii to depressive rats. *Frontiers in Pharmacology* 9:131
50. Tao Y, Yu Q, Huang Y, Liu R, Zhang X, et al. 2022. Identification of crucial polymethoxyflavones tangeretin and 3,5,6,7,8,3',4'-heptamethoxyflavone and evaluation of their contribution to anticancer effects of *Pericarpium Citri reticulatae* 'Chachi' during storage. *Antioxidants* 11(10):1922
51. Wang J, Li G, Li C, Zhang C, Cui L, et al. 2021. NF-Y plays essential roles in flavonoid biosynthesis by modulating histone modifications in tomato. *New Phytologist* 229:3237–52
52. Dong NQ, Lin HX. 2021. Contribution of phenylpropanoid metabolism to plant development and plant-environment interactions. *Journal of Integrative Plant Biology* 63:180–209
53. Hichri I, Barrieu F, Bogs J, Kappel C, Delrot S, et al. 2011. Recent advances in the transcriptional regulation of the flavonoid biosynthetic pathway. *Journal of Experimental Botany* 62(8):2465–83
54. Xing A, Wang X, Nazir MF, Zhang X, Wang X, et al. 2022. Transcriptomic and metabolomic profiling of flavonoid biosynthesis provides novel insights into petals coloration in Asian cotton (*Gossypium arboreum* L.). *BMC Plant Biology* 22:416
55. Nabavi SM, Dunja Š, Tomczyk M, Milella L, Russo D, et al. 2020. Flavonoid biosynthetic pathways in plants: versatile targets for metabolic engineering. *Biotechnology Advances* 38:107316
56. Zhao T, Li R, Yao W, Wang Y, Zhang C, et al. 2021. Genome-wide identification and characterisation of phenylalanine ammonia-lyase gene family in grapevine. *The Journal of Horticultural Science and Biotechnology* 96(4):456–68
57. Barros J, Dixon RA. 2020. Plant phenylalanine/tyrosine ammonia-lyases. *Trends in Plant Science* 25:66–79
58. Cheng GW, Breen PJ. 1991. Activity of Phenylalanine Ammonia-Lyase (PAL) and concentrations of anthocyanins and phenolics in developing strawberry fruit. *Journal of the American Society for Horticultural Science jashs* 116:865–69

59. Lu C, Yan X, Zhang H, Zhong T, Gui A, et al. 2024. Integrated metabolomic and transcriptomic analysis reveals biosynthesis mechanism of flavone and caffeoylquinic acid in chrysanthemum. *BMC Genomics* 25:759
60. Li Y, Kim JI, Pysh L, Chapple C. 2015. Four isoforms of arabidopsis 4-coumarate: CoA ligase have overlapping yet distinct roles in phenylpropanoid metabolism. *Plant Physiology* 169:2409–21
61. Pietrowska-Borek M, Chadzinikolau T, Kozłowska M. 2010. Effect of urban pollution on 4-coumarate: CoA ligase and flavonoid accumulation in Berberis thunbergii. *Dendrobiology* 64:79–85
62. Deng X, Bashandy H, Ainasoja M, Kontturi J, Pietiäinen M, et al. 2014. Functional diversification of duplicated chalcone synthase genes in anthocyanin biosynthesis of *Gerbera hybrida*. *New Phytologist* 201:1469–83
63. Yin YC, Zhang XD, Gao ZQ, Hu T, Liu Y. 2019. The research progress of chalcone isomerase (CHI) in plants. *Molecular Biotechnology* 61:32–52
64. Schijlen EGWM, de Vos CH, Martens S, Jonker HH, Rosin FM, et al. 2007. RNA interference silencing of chalcone synthase, the first step in the flavonoid biosynthesis pathway, leads to parthenocarpic tomato fruits. *Plant Physiology* 144:1520–30
65. Jiang W, Yin Q, Wu R, Zheng G, Liu J, et al. 2015. Role of a chalcone isomerase-like protein in flavonoid biosynthesis in Arabidopsis thaliana. *Journal of Experimental Botany* 66:7165–7179
66. Zhu J, Zhao W, Li R, Guo D, Li H, et al. 2021. Identification and characterization of chalcone isomerase genes involved in flavonoid production in *Dracaena cambodiana*. *Frontiers in Plant Science* 12:616396
67. Li H, Lv Q, Ma C, Qu J, Cai F, et al. 2019. Metabolite profiling and transcriptome analyses provide insights into the flavonoid biosynthesis in the developing seed of tartary buckwheat (Fagopyrum tataricum). *Journal of Agricultural and Food Chemistry* (40): 11262-76
68. Weber B, Hartmann B, Stöckigt D, Schreiber K, Roloff M, et al. 2006. Liquid chromatography mass spectrometry and liquid chromatography/nuclear magnetic resonance as complementary analytical techniques for unambiguous identification of polymethoxylated flavones in residues from molecular distillation of orange peel oils (*Citrus sinensis*). *Journal of Agricultural and Food Chemistry* 54(2):274–78
69. Saini RK, Ranjit A, Sharma K, Prasad P, Shang X, et al. 2022. Bioactive compounds of Citrus fruits: a review of composition and health benefits of carotenoids, flavonoids, limonoids, and terpenes. *Antioxidants* 11(2):239
70. Liao Z, Liu X, Zheng J, Zhao C, Wang D, et al. 2023. A multifunctional true caffeoyl coenzyme A O-methyltransferase enzyme participates in the biosynthesis of polymethoxylated flavones in citrus. *Plant Physiology* 192(3):2049–66
71. Alseekh S, Perez de Souza L, Benina M, Fernie AR. 2020. The style and substance of plant flavonoid decoration; towards defining both structure and function. *Phytochemistry* 174:112347
72. Liu Y, Fernie AR, Tohge T. 2022. Diversification of chemical structures of methoxylated flavonoids and genes encoding flavonoid-O-methyltransferases. *Plants* 11:564
73. Zohra FT, Takematsu S, Yuri I, Nobuhiro K. 2020. Accumulation of polymethoxyflavones and *O*-methyltransferase gene expression in various citrus cultivars. *Horticulture Journal* 89:225–36
74. Berim A, Gang DR. 2016. Methoxylated flavones: occurrence, importance, biosynthesis. *Phytochemistry Reviews* 15:363–90